

General variational approach to nuclear-quadrupole coupling in rovibrational spectra of polyatomic molecules

Andrey Yachmenev^{1,2,a)} and Jochen Küpper^{1,2,3}

¹⁾Center for Free-Electron Laser Science, Deutsches Elektronen-Synchrotron DESY, Notkestrasse 85, 22607 Hamburg, Germany

²⁾The Hamburg Center for Ultrafast Imaging, Universität Hamburg, Luruper Chaussee 149, 22761 Hamburg, Germany

³⁾Department of Physics, Universität Hamburg, Luruper Chaussee 149, 22761 Hamburg, Germany

(Dated: 7 March 2024)

A general algorithm for computing the quadrupole-hyperfine effects in the rovibrational spectra of polyatomic molecules is presented for the case of ammonia (NH₃). The method extends the general variational approach TROVE by adding the extra term in the Hamiltonian that describes the nuclear quadrupole coupling, with no inherent limitation on the number of quadrupolar nuclei in a molecule. We applied the new approach to compute the nitrogen-nuclear-quadrupole hyperfine structure in the rovibrational spectrum of ¹⁴NH₃. These results agree very well with recent experimental spectroscopic data for the pure rotational transitions in the ground vibrational and ν_2 states, and the rovibrational transitions in the ν_1 , ν_3 , $2\nu_4$, and $\nu_1 + \nu_3$ bands. The computed hyperfine-resolved rovibrational spectrum of ammonia will be beneficial for the assignment of experimental rovibrational spectra, further detection of ammonia in interstellar space, and studies of the proton-to-electron mass variation.

Precision spectroscopy of small molecules promises new windows into fundamental physics,¹ but requires a detailed understanding of their complex energy-level structures, including the hyperfine structure due to the interaction between the rovibronic molecular states and the nuclear spins of their constituent atoms. Recent advances in high-resolution sub-Doppler spectroscopy and astronomical observations of interstellar environments have also triggered renewed interest in the hyperfine-structure of molecular spectra. For instance, the hyperfine structure of molecular rovibrational energy levels is relevant for a variety of applications in precision spectroscopy,^{2,3} ultracold chemical reactions,^{4–7} highly correlated quantum gases,^{8–11} and quantum-information processing.^{12,13} Shifts of the hyperfine-split energy levels and transition frequencies in time can serve as useful probe for testing whether there is any cosmological variability of the proton-to-electron mass ratio,^{14–17} predicted by theories beyond the Standard Model. Even for spectra with Doppler-limited resolution, detailed knowledge of the hyperfine patterns of rovibrational energy levels is very useful for determining the absolute line positions and verifying the spectroscopic assignments.¹⁸

So far the hyperfine structure of rovibrational energy levels is described using effective Hamiltonian models,^{19,20} with only a few exceptions.^{21–23} However, due to the scantness of hyperfine-resolved spectroscopic data, the effective Hamiltonian approaches are very limited in extrapolating to energy levels that are not directly experimentally sampled. For accurate predictions over a broader spectral range it is highly desirable to employ variational approaches, which show much better extrapolation properties than the effective-Hamiltonian

approaches, e. g., because they intrinsically incorporate all resonant interactions between rovibrational states. Over the last decade, a considerable amount of work has been put into the development of such variational approaches and their efficient computer implementations.^{24–31} TROVE^{25,31} is a general black-box computational paradigm for calculating the rovibrational energy levels of polyatomic molecules in isolated electronic states. It is based on a completely numerical approach for computing the Hamiltonian matrix and solving the eigenvalue problem. Along with its algorithmic efficiency, TROVE benefits from the use of molecular symmetry, including non-Abelian symmetry groups,³² curvilinear internal coordinates and the Eckart coordinate frame.³¹ Over the last few years TROVE has actively been employed for computing comprehensive rovibrational line lists for a number of polyatomic molecules important for modeling and characterisation of cool stars and exoplanets.³³

Here, we extend TROVE to include hyperfine effects at the level of the nuclear-quadrupole coupling. The coupling is described by the interaction of the nuclear quadrupole moments with the electric field gradient at the nuclei. The latter is treated as a function of the nuclear internal coordinates and we impose no inherent limitations on the number of internal degrees of freedom nor the number of quadrupolar nuclei. Thus, it is applicable to molecules with arbitrary structure. To our knowledge, this work is the first attempt to create a general approach for computing nuclear spin effects with high accuracy based on the robust variational method.

We apply the newly developed method to compute the rovibrational spectrum of NH₃ with resolved hyperfine quadrupole structure. We use existing accurate potential energy and electric dipole moment surfaces of NH₃^{34,35} along with a newly *ab initio* calculated electric field gradient tensor surface. Small empirical corrections were added to the calculated spin-free vibrational band centers

^{a)}Electronic mail: andrey.yachmenev@cfel.de; <https://www.controlled-molecule-imaging.org>

to match the experimentally derived energies from the MARVEL database.³⁶ The resulting calculated data are in very good agreement with the available experimental quadrupole splittings for the ground vibrational state³⁷ and the excited vibrational states ν_2 ,³⁸ ν_1 , ν_3 , and $2\nu_4$ ³⁹ as well as with the hyperfine splittings and intensities of recent sub-Doppler spectral measurements for the $\nu_1 + \nu_3$ band.¹⁸ We expect that our results will aid the spectroscopic analysis of many unassigned overlapping rovibrational features in the spectrum of $^{14}\text{NH}_3$ and support astronomical detection of ammonia in interstellar media. The results are also relevant for future laboratory and astronomical observations of the proton-to-electron mass variation.^{14,16}

Within the Born-Oppenheimer approximation the quadrupole structure of the rovibrational energy levels in a molecule containing $l = 1 \dots N$ quadrupolar nuclei is described by the coupling of the electric field gradient (EFG) at each l th nucleus $\mathbf{V}(l)$ with its quadrupole moment $\mathbf{Q}(l)$ ⁴⁰

$$H_{\text{qc}} = \sum_l^N \mathbf{V}(l) \cdot \mathbf{Q}(l). \quad (1)$$

The operator $\mathbf{V}(l)$ acts only on the rovibrational coordinates and momenta of the nuclei, while the operator $\mathbf{Q}(l)$ depends solely on the nuclear spin angular momenta and fine-structure constants. The total spin-rovibrational wave functions $|F, m_F\rangle$ can be constructed from the linear combinations of products of the rovibrational wave functions $|J, m_J, w\rangle$ and the nuclear spin functions $|I, m_I, \mathcal{I}\rangle$. Here, J , I , and F denote the quantum numbers of the rotational \mathbf{J} , collective nuclear spin \mathbf{I} , and total angular momentum $\mathbf{F} = \mathbf{J} + \mathbf{I}$ operators, respectively. m_J , m_I , and m_F denote the quantum numbers of the corresponding laboratory-frame projections, and w and \mathcal{I} stand for the sets of additional quanta characterizing rovibrational and nuclear spin states, respectively. The matrix representation of the quadrupole-coupling Hamiltonian in a basis of functions $|F, m_F\rangle$ is diagonal in F and m_F and can be expressed as

$$\begin{aligned} \langle F, m_F | H_{\text{qc}} | F, m_F \rangle &= (-1)^{J+I+F} \begin{Bmatrix} F & I' & J' \\ 2 & J & I \end{Bmatrix} \\ &\times \sum_l^N \langle J', w' | V^{(2)}(l) | J, w \rangle \cdot \langle I', \mathcal{I}' | Q^{(2)}(l) | I, \mathcal{I} \rangle, \quad (2) \end{aligned}$$

where $V^{(2)}(l)$ and $Q^{(2)}(l)$ are the EFG and the quadrupole moment operators in the irreducible tensor form.

For $N > 1$ quadrupolar nuclei with spins I_1, I_2, \dots, I_N , the nuclear spin basis functions $|I, m_I, \mathcal{I}\rangle$ are unambiguously characterized by the set of quantum numbers $\mathcal{I} = \{I_{12}, I_{13}, \dots, I_{1N-1}\}$ and $I \equiv I_{1N}$ denoting the eigenstates of the coupled spin angular momenta $\mathbf{I}_{12} = \mathbf{I}_1 + \mathbf{I}_2$, $\mathbf{I}_{13} = \mathbf{I}_{12} + \mathbf{I}_3, \dots, \mathbf{I}_{1N-1} = \mathbf{I}_{1N-2} + \mathbf{I}_{N-1}$ and $\mathbf{I}_{1N} = \mathbf{I}_{1N-1} + \mathbf{I}_N$, respectively. For $N = 1$, the quantum number \mathcal{I} is omitted. In this basis, the reduced matrix elements of the

quadrupole moment operator $Q^{(2)}(l)$ can be expressed as

$$\langle I', \mathcal{I}' | Q^{(2)}(l) | I, \mathcal{I} \rangle = \frac{1}{2} (eQ_l) C_l^{(I' \mathcal{I}', I \mathcal{I})} \begin{pmatrix} I_l & 2 & I_l \\ -I_l & 0 & I_l \end{pmatrix}^{-1} \quad (3)$$

where (eQ_l) stands for the nuclear quadrupole constant and the explicit expression for the coupling coefficients $C_l^{(I' \mathcal{I}', I \mathcal{I})}$ is given in the supplementary material.⁴¹

The reduced matrix elements of the EFG operator $V^{(2)}(l)$ are given by the expression

$$\begin{aligned} \langle J', w' | V^{(2)}(l) | J, w \rangle &= \frac{1}{2} (-1)^{J-J'} \begin{pmatrix} J' & 2 & J \\ -J & 0 & J \end{pmatrix}^{-1} \\ &\times \langle J', m_J' = J, w' | V_{ZZ}(l) | J, m_J = J, w \rangle, \quad (4) \end{aligned}$$

where V_{ZZ} is the (Z, Z) -component of the EFG tensor in the laboratory frame and $m_J' = m_J = \min(J, J')$.

The rovibrational wave functions $|J, m_J, w\rangle$ and energies $E_{J,w}$ are obtained from TROVE calculations and are represented by linear combinations of pure vibrational $|v\rangle$ and symmetric top $|J, m_J, k, \tau\rangle$ wavefunctions

$$|J, m_J, w\rangle = \sum_{k\tau v} C_{k\tau v}^{(J,w)} |v\rangle |J, m_J, k, \tau\rangle, \quad (5)$$

where $k = 0 \dots J$; $\tau = 0$ or 1 defines rotational parity as $(-1)^\tau$, and $C_{k\tau v}^{(J,w)}$ are the eigenvector coefficients of the total rovibrational Hamiltonian. To compute the matrix elements of V_{ZZ} in (4) in the basis of the rovibrational functions given by (5), we employ a general approach:⁴²

$$\langle J', m_J', w' | V_{ZZ}(l) | J, m_J, w \rangle = \mathcal{M}_2^{(J' m_J', J m_J)} \mathcal{K}_2^{(J' w', J w)}(l), \quad (6)$$

with

$$\begin{aligned} \mathcal{M}_2^{(J' m_J', J m_J)} &= (-1)^{m_J'} \sqrt{(2J' + 1)(2J + 1)} \\ &\times \sum_{\sigma=-2}^2 [T^{(2)}]_{ZZ, \sigma}^{-1} \begin{pmatrix} J & 2 & J' \\ m_J & \sigma & -m_J' \end{pmatrix} \quad (7) \end{aligned}$$

and

$$\begin{aligned} \mathcal{K}_2^{(J' w', J w)}(l) &= \sum_{\substack{k' \tau' v' \\ k \tau v}} [C_{k' \tau' v'}^{(J', w')}]^* C_{k \tau v}^{(J, w)} \sum_{\pm k', \pm k} [c_{k'}^{(\tau')}]^* c_k^{(\tau)} \\ &\times (-1)^{k'} \sum_{\sigma=-2}^2 \sum_{\alpha \leq \beta} \begin{pmatrix} J & 2 & J' \\ k & \sigma & -k' \end{pmatrix} T_{\sigma, \alpha \beta}^{(2)} \langle v' | \bar{V}_{\alpha \beta}(l) | v \rangle. \quad (8) \end{aligned}$$

Here, $\bar{V}_{\alpha \beta}(l)$ ($\alpha, \beta = x, y, z$) denotes the EFG tensor in the molecular frame, the constant 5×6 matrix $\mathbf{T}^{(2)}$ and its inverse are the forward and backward transformation, respectively, of the traceless second-rank Cartesian tensor operator into its spherical tensor representation, and $c_{\pm k}^{(\tau)}$

are the so-called Wang transformation coefficients defining $|J, m_J, k, \tau\rangle = c_{+k}^{(\tau)} |J, m_J, k\rangle + c_{-k}^{(\tau)} |J, m_J, -k\rangle$. Explicit expressions for $T^{(2)}$ and $c_{\pm k}^{(\tau)}$ are given in the supplementary material.⁴¹

The computational procedure can be summarized as following: First we variationally solve the spin-free rovibrational problem with TROVE and obtain the rovibrational energies $E_{J,w}$ and wave functions $|J, m_J, w\rangle$ according to (5) for states with $J = 0 \dots J_{\max}$ and energies $E_{J,w}$ below a given threshold. The *ab initio* computed values of the EFG tensor $\bar{V}_{\alpha\beta}(l)$ at various molecular geometries are obtained from a least-squares fit by a truncated power series expansions in terms of the internal coordinates of the molecule. In the next step, the matrix elements $\mathcal{K}_2(l)$ in (8) are evaluated for the desired rovibrational states for all quadrupolar nuclei l and stored in a database format similar to that adopted for spectroscopic line lists.³³ The matrix elements of H_{qc} in (2) can efficiently be assembled on the fly from the products of the compact $\mathcal{K}_2(l)$ and \mathcal{M}_2 matrices together with the reduced matrix elements of the quadrupole moment operator, given by (3). The spin-rovibrational energies and wave functions are obtained by solving the eigenvalue problem for the total Hamiltonian, which is the sum of the diagonal representation of the pure rovibrational Hamiltonian $E_{J,w} \delta_{I',I} \delta_{l',l}$ and the non-diagonal matrix representation of H_{qc} . Since the H_{qc} operator commutes with all operations of the molecular symmetry group, it factorizes into independent blocks for each symmetry, which are processed separately. The relevant equations for the dipole transition line strengths and notes on the computer implementation are presented in the supplementary material.⁴¹

Now, we apply the developed method to compute the hyperfine quadrupole structure in the rovibrational spectrum of $^{14}\text{NH}_3$. To compute the spin-free rovibrational states we used the approach described in a previous study that generated an extensive rovibrational line list of NH_3 .⁴³ We used the available spectroscopically refined potential energy surface (PES)³⁴ and *ab initio* dipole moment surface³⁵ of NH_3 and truncated the vibrational basis set at the polyad number $P = 14$.

The EFG tensor $\bar{V}_{\alpha\beta}$ at the quadrupolar nucleus ^{14}N was computed on a grid of 4700 different symmetry-independent molecular geometries of NH_3 employing the CCSD(T) level of theory in the frozen-core approximation and the aug-cc-pVQZ basis set.^{44,45} Calculations were performed using analytical coupled cluster energy derivatives,⁴⁶ as implemented in the CFOUR program package.⁴⁷ To represent each element of the $\bar{V}_{\alpha\beta}$ tensor analytically, in terms of internal coordinates of NH_3 , we first transformed it into a symmetry-adapted form under

the $\mathbf{D}_{3h}(\text{M})$ molecular symmetry group, as

$$V_1^{(A'_1)} = V_{44}, \quad (9)$$

$$V_2^{(E'_a)} = (2V_{12} - V_{13} - V_{23})/\sqrt{6}, \quad (10)$$

$$V_2^{(E'_b)} = (V_{13} - V_{23})/\sqrt{2}, \quad (11)$$

$$V_3^{(E''_a)} = (2V_{14} - V_{24} - V_{34})/\sqrt{6}, \quad (12)$$

$$V_3^{(E''_b)} = (V_{24} - V_{34})/\sqrt{2}. \quad (13)$$

Since the EFG tensor is traceless, the totally symmetric combination $V^{(A'_1)} = (V_{11} + V_{22} + V_{33})/\sqrt{3} = 0$ vanishes. V_{ij} ($i, j = 1 \dots 4$) denote projections of the $\bar{V}_{\alpha\beta}$ Cartesian tensor onto a system of four molecular-bond unit vectors, defined as following³⁵

$$\mathbf{e}_i = (\mathbf{r}_{\text{H}_i} - \mathbf{r}_{\text{N}})/r_{\text{NH}_i} \quad \text{for } i = 1, 2, 3 \quad (14)$$

$$\mathbf{e}_4 = \frac{\mathbf{e}_1 \times \mathbf{e}_2 + \mathbf{e}_2 \times \mathbf{e}_3 + \mathbf{e}_3 \times \mathbf{e}_1}{\|\mathbf{e}_1 \times \mathbf{e}_2 + \mathbf{e}_2 \times \mathbf{e}_3 + \mathbf{e}_3 \times \mathbf{e}_1\|}, \quad (15)$$

where \mathbf{r}_{H_i} and \mathbf{r}_{N} are the instantaneous Cartesian coordinates of the hydrogen and nitrogen nuclei and r_{NH_i} are the N–H_{*i*} internuclear distances. The E_a and E_b symmetry components of the doubly degenerate representations E' and E'' are connected by a simple orthogonal transformation and can be parametrized by one set of constants. The remaining three symmetry-unique combinations $V_1^{(A'_1)}$, $V_2^{(E'_a)}$, and $V_3^{(E''_a)}$ were parametrized by the symmetry-adapted power series expansions to sixth order using the least squares fitting. The values of the optimized parameters and the Fortran 90 functions for computing $V_i^{(\Gamma)}$ in (9)–(13) are provided in the supplementary material.⁴¹

The computed rovibrational line list for $^{14}\text{NH}_3$ covers all states with $F \leq 15$ ($F = |J - I_{\text{N}}| \dots J + I_{\text{N}}$ and $I_{\text{N}} = 1$) and energies $E_{J,w} \leq 8000 \text{ cm}^{-1}$ relative to the zero-point level. A value of $eQ = 20.44 \text{ mb}$ for the ^{14}N nuclear quadrupole constant was used.⁴⁸

In Figure 1 we compare the predicted quadrupole hyperfine transition frequencies for NH_3 with the available experimental data. We have chosen the most recent and easily digitized experimental data sets, which contain rotational transitions in the ground vibrational³⁷ and ν_2 ³⁸ states, and rovibrational transitions from the ground to the ν_1 , $\nu_3^{\pm 1}$, $2\nu_4^0$, and $2\nu_4^{\pm 2}$ vibrational states.³⁹ An extended survey of the published experimental and theoretical data for the quadrupole hyperfine structure of ammonia can be found elsewhere.^{39,49} The absolute errors in the rovibrational frequencies, plotted with circles, are within the accuracy of the underlying PES.³⁴ To estimate the accuracy of the predicted quadrupole splittings, we subtracted the respective error in the rovibrational frequency unperturbed from the quadrupole interaction effect for each transition. The resulting errors, plotted with stars in Figure 1, range from 0.1 to 25 kHz for the ground vibrational state and from 2.6 to 64 kHz for the ν_2 state. These values correspond to the maximal

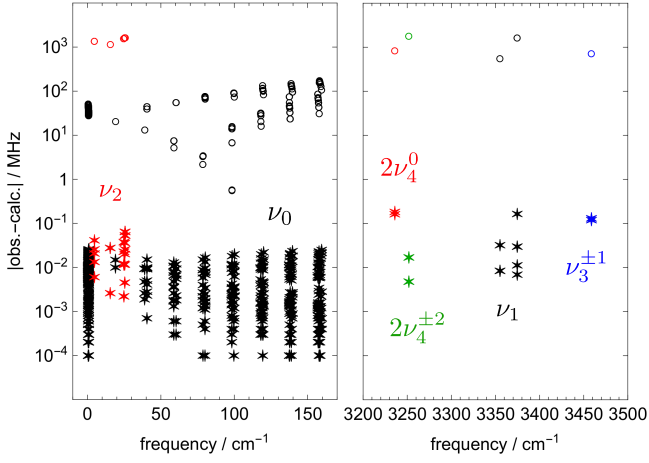


FIG. 1. Absolute values of the discrepancies of the calculated transition frequencies of NH_3 to the experimental data for (left panel) the ground ν_0 and ν_2 vibrational states and (right panel) the ν_1 , $\nu_3^{\pm 1}$, $2\nu_4^0$, $2\nu_4^{\pm 2}$ bands. The errors in the rovibrational frequencies are plotted with circles while the relative errors of the quadrupole splittings are plotted with stars.

relative errors in computed hyperfine splittings of 0.6 % and 1.4 % for the ground and ν_2 states, respectively. For other fundamental and overtone bands,⁵⁰ these errors are bigger, up to 160 kHz (3.9 %), however, the estimated uncertainty of the experimental data already accounts for ± 100 (2.4 %) kHz.³⁹

We believe that the accuracy of the quadrupole splittings can be significantly improved by employing a better level of the electronic structure theory in the calculations of the EFG surface. For example, the aug-cc-pVQZ basis set incompleteness error and the core electron correlation effects were shown to contribute up to 0.004 a.u. and 0.01 a.u., respectively, into the absolute values of the EFG tensor of the water molecule.⁵¹ By scaling these values with the nuclear quadrupole constant of the ^{14}N atom, we estimate that the electronic structure errors in the quadrupole splittings of ammonia are as large as 50 kHz.

In Figure 2 we compare our results with sub-Doppler saturation-dip spectroscopic measurements for the $\nu_1 + \nu_3$ band of NH_3 .¹⁸ The saturation-dip lineshapes were calculated as the intensity-weighted sums of Lorentzian-lineshape derivatives⁵² with a half-width-at-half-maximum (HWHM) width of the absorption profile of 290 kHz and the HWHM-amplitude of the experimentally applied frequency-modulation dither of 150 kHz.⁵³ The $^pP(5, K_a'')$ transitions were recorded with slightly larger HWHM⁵³ and we found a value of 500 kHz to best reproduce the measured lineshapes for these transitions. The computed profiles for $^rP(3, 0)_s$, $^pP(2, 1)_s$, $^pP(5, 3)_s$, and $^pP(5, 4)_s$ transitions show very good agreement with the measurement. For $^pP(5, 3)_a$ and $^pP(5, 4)_a$ transitions the calculated profiles do not match the experiment very well. In the experimental work,¹⁸ the predicted double peak feature of the $^pP(5, 3)_a$ was not observed while for

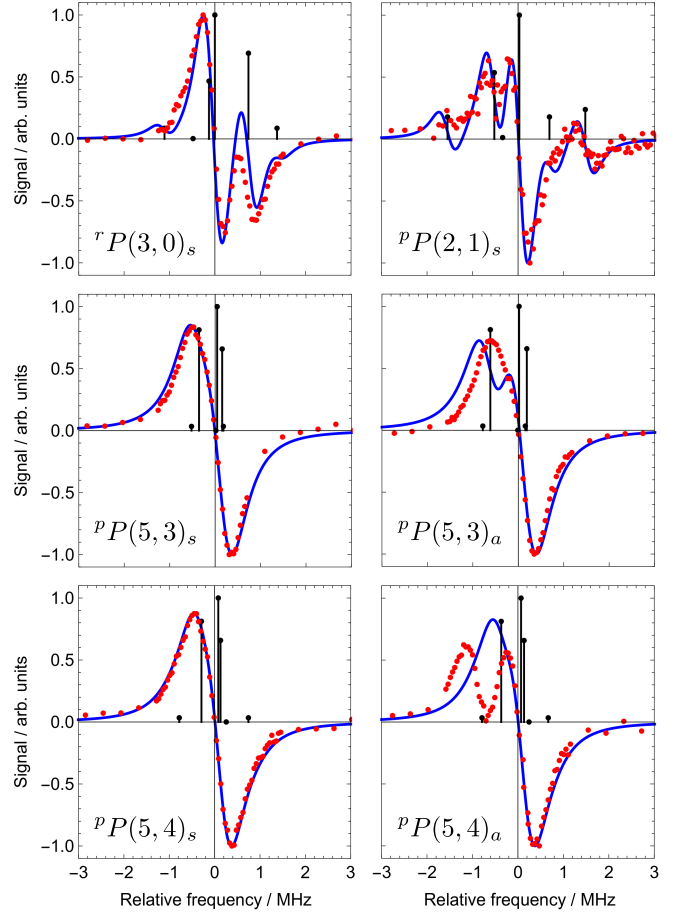


FIG. 2. Comparison of the calculated (blue line) and observed¹⁸ (red dots) saturation dip line shapes for $\Delta K_a \Delta J(J'', K_a'')\tau''_{\text{inv}}$ transitions of the $\nu_1 + \nu_3$ band of NH_3 ($\tau''_{\text{inv}} = s$ or a denotes *symmetric* or *anti-symmetric* inversion parity of the ground vibrational state). Stems show contributing to the calculated line shape stick spectrum. The experimental and calculated intensities are normalized to the respective maximal values. The measured (calculated) zero-crossing wavenumbers, in cm^{-1} , are 6544.32154 (6544.49333) for $^rP(3, 0)_s$, 6572.85349 (6572.87926) for $^pP(2, 1)_s$, 6529.18969 (6530.047789) for $^pP(5, 3)_s$, 6528.76857 (6528.51408) for $^pP(5, 3)_a$, 6536.59280 (6537.31784) for $^pP(5, 4)_s$, and 6537.68063 (6536.68512) for $^pP(5, 4)_a$.

the $^pP(5, 4)_a$ it was attributed to perturbations. Based on the results of the present variational calculations the latter can not be confirmed. It should be noted, however, that the accuracy of the underlying PES is not sufficiently high in this energy region at $1.5 \mu\text{m}$ to unambiguously match the predicted rovibrational frequencies with the measured ones. Moreover, the PES employed here was obtained by a refinement of the *ab initio* surface to the high resolution spectroscopic data of NH_3 . It is well known, that the PES refinement may cause appearance of the spurious intensity borrowing effects as well as dissipation of the true accidental resonances in various regions of the spectrum.^{54,55} Therefore, we refrain here

from discussion of the possible alternative assignment of the $^pP(5,3)_a$ and $^pP(5,4)_a$ transitions. Calculations of a new, more accurate PES of NH_3 are currently performed and analyzed,⁵⁶ which, once available, will be used to generate a more accurate quadrupole-hyperfine-resolved spectrum.

In conclusion, we have presented the first general-molecule variational implementation of nuclear-quadrupole hyperfine effects. Our approach is based on TROVE, which provides accurate spin-free rovibrational energy levels and wave functions used as a basis for the quadrupole-coupling problem. The initial results for $^{14}\text{NH}_3$ are in very good agreement with the available experimental data. The generated rovibrational line list for $^{14}\text{NH}_3$ with quadrupole-coupling components is available as part of the supplementary material.⁴¹ We believe that computed hyperfine-resolved rovibrational spectrum of ammonia will be beneficial for the assignment of high resolution measurements in the near-infrared.

Calculations based on more accurate PES and the extension of the present approach to incorporate the hyperfine effects due to the spin-spin and spin-rotation couplings are currently performed in our group. Due to the general approach, predictions of similar quality will be possible for other small polyatomic molecules in order to guide future laboratory and astronomical observations with sub-Doppler resolution, including investigations of *para-ortho* transitions^{23,57} or proton-to-electron-mass variations.^{14,17}

We gratefully acknowledge Trevor Sears for providing us with their original experimental data.¹⁸ Besides DESY, this work has been supported by the excellence cluster “The Hamburg Center for Ultrafast Imaging—Structure, Dynamics and Control of Matter at the Atomic Scale” of the Deutsche Forschungsgemeinschaft (CUI, DFG-EXC1074).

- ¹D. DeMille, “Diatomic molecules, a window onto fundamental physics,” *Phys. Today* **68**, 34–40 (2015).
- ²H. L. Bethlem, M. Kajita, B. Sartakov, G. Meijer, and W. Ubachs, “Prospects for precision measurements on ammonia molecules in a fountain,” *Eur. Phys. J. Special Topics* **163**, 55–69 (2008).
- ³M. Schnell and J. Küpper, “Tailored molecular samples for precision spectroscopy experiments,” *Faraday Disc.* **150**, 33–49 (2011).
- ⁴M. T. Bell and T. P. Softley, “Ultracold molecules and ultracold chemistry,” *Mol. Phys.* **107**, 99–132 (2009).
- ⁵S. Y. T. van de Meerakker, H. L. Bethlem, N. Vanhaecke, and G. Meijer, “Manipulation and control of molecular beams,” *Chem. Rev.* **112**, 4828–4878 (2012).
- ⁶C. Naulin and M. Costes, “Experimental search for scattering resonances in near cold molecular collisions,” *Int. Rev. Phys. Chem.* **33**, 427–446 (2014).
- ⁷B. K. Stuhl, M. T. Hummon, and J. Ye, “Cold state-selected molecular collisions and reactions,” *Annu. Rev. Phys. Chem.* **65**, 501–518 (2014).
- ⁸M. A. Baranov, M. Dalmon, G. Pupillo, and P. Zoller, “Condensed matter theory of dipolar quantum gases,” *Chem. Rev.* **112**, 5012–5061 (2012).
- ⁹S. Ospelkaus, K.-K. Ni, G. Quémener, B. Neyenhuis, D. Wang, M. H. G. de Miranda, J. L. Bohn, J. Ye, and D. S. Jin, “Controlling the hyperfine state of rovibronic ground-state polar molecules,” *Phys. Rev. Lett.* **104**, 030402 (2010).
- ¹⁰J. Aldegunde, H. Ran, and J. M. Hutson, “Manipulating ultracold

polar molecules with microwave radiation: The influence of hyperfine structure,” *Phys. Rev. A* **80**, 043410 (2009).

- ¹¹S. A. Moses, J. P. Covey, M. T. Miecikowski, D. S. Jin, and J. Ye, “New frontiers for quantum gases of polar molecules,” *Nat. Phys.* **13**, 13–20 (2016).
- ¹²Q. Wei, S. Kais, B. Friedrich, and D. Herschbach, “Entanglement of polar symmetric top molecules as candidate qubits,” *J. Chem. Phys.* **135**, 154102 (2011).
- ¹³A. Jaouadi, E. Barrez, Y. Justum, and M. Desouter-Lecomte, “Quantum gates in hyperfine levels of ultracold alkali dimers by revisiting constrained-phase optimal control design,” *J. Chem. Phys.* **139**, 014310 (2013).
- ¹⁴J. van Veldhoven, J. Küpper, H. L. Bethlem, B. Sartakov, A. J. A. van Roij, and G. Meijer, “Decelerated molecular beams for high-resolution spectroscopy: The hyperfine structure of $^{15}\text{ND}_3$,” *Eur. Phys. J. D* **31**, 337–349 (2004).
- ¹⁵V. V. Flambaum and M. G. Kozlov, “Limit on the cosmological variation of $m(p)/m(e)$ from the inversion spectrum of ammonia,” *Phys. Rev. Lett.* **98**, 240801 (2007).
- ¹⁶A. Owens, S. N. Yurchenko, W. Thiel, and V. Špirko, “Enhanced sensitivity to a possible variation of the proton-to-electron mass ratio in ammonia,” *Phys. Rev. A* **93**, 052506 (2016).
- ¹⁷C. Cheng, A. P. P. van der Poel, P. Jansen, M. Quintero-Pérez, T. E. Wall, W. Ubachs, and H. L. Bethlem, “Molecular fountain,” *Phys. Rev. Lett.* **117**, 253201 (2016).
- ¹⁸S. Twagirayezu, G. E. Hall, and T. J. Sears, “Quadrupole splittings in the near-infrared spectrum of $^{14}\text{NH}_3$,” *J. Chem. Phys.* **145**, 144302 (2016).
- ¹⁹J. T. Hougen, “Reinterpretation of molecular beam hyperfine data for $^{14}\text{NH}_3$ and $^{15}\text{NH}_3$,” *J. Chem. Phys.* **57**, 4207–4217 (1972).
- ²⁰W. Gordy and R. L. Cook, *Microwave Molecular Spectra*, 3rd ed. (John Wiley & Sons, New York, NY, USA, 1984).
- ²¹P. Jensen, I. Paidarová, J. Vojtk, and V. Špirko, “Theoretical calculations of the nuclear quadrupole coupling in the spectra of D_3^+ , H_2D^+ , and HD_2^+ ,” *J. Mol. Spec.* **150**, 137–163 (1991).
- ²²P. Jensen and S. P. A. Sauer, “Theoretical calculations of the hyperfine structure in the spectra of H_3^+ and its deuterated isotopomers,” *Mol. Phys.* **91**, 319–332 (1997).
- ²³A. Miani and J. Tennyson, “Can ortho-para transitions for water be observed?” *J. Chem. Phys.* **120**, 2732–2739 (2004).
- ²⁴D. Lauvergnat and A. Nauts, “Exact numerical computation of a kinetic energy operator in curvilinear coordinates,” *J. Chem. Phys.* **116**, 8560 (2002).
- ²⁵S. N. Yurchenko, W. Thiel, and P. Jensen, “Theoretical ROVibrational energies (TROVE): A robust numerical approach to the calculation of rovibrational energies for polyatomic molecules,” *J. Mol. Spec.* **245**, 126–140 (2007).
- ²⁶E. Mátyus, G. Czako, B. T. Sutcliffe, and A. G. Császár, “Vibrational energy levels with arbitrary potentials using the Eckart-Watson Hamiltonians and the discrete variable representation,” *J. Chem. Phys.* **127**, 084102 (2007).
- ²⁷E. Mátyus, G. Czako, and A. G. Császár, “Toward black-box-type full- and reduced-dimensional variational (ro)vibrational computations,” *J. Chem. Phys.* **130**, 134112 (2009).
- ²⁸X.-G. Wang and T. Carrington, “A discrete variable representation method for studying the rovibrational quantum dynamics of molecules with more than three atoms,” *J. Chem. Phys.* **130**, 094101 (2009).
- ²⁹G. Avila and T. Carrington, “Solving the Schrödinger equation using smolyak interpolants,” *J. Chem. Phys.* **139**, 134114 (2013).
- ³⁰C. Fábri, E. Mátyus, and A. G. Császár, “Rotating full- and reduced-dimensional quantum chemical models of molecules,” *J. Chem. Phys.* **134**, 074105 (2011).
- ³¹A. Yachmenev and S. N. Yurchenko, “Automatic differentiation method for numerical construction of the rotational-vibrational Hamiltonian as a power series in the curvilinear internal coordinates using the Eckart frame,” *J. Chem. Phys.* **143**, 014105 (2015).
- ³²S. N. Yurchenko, A. Yachmenev, and R. I. Ovsyannikov, “Symmetry adapted ro-vibrational basis functions for variational nuclear motion

- calculations: TROVE approach," *J. Chem. Theory Comput.* (2017), 10.1021/acs.jctc.7b00506, accepted.
- ³³J. Tennyson, S. N. Yurchenko, A. F. Al-Refaie, E. J. Barton, K. L. Chubb, P. A. Coles, S. Diamantopoulou, M. N. Gorman, C. Hill, A. Z. Lam, L. Lodi, L. K. McKemmish, Y. Na, A. Owens, O. L. Polyansky, T. Rivlin, C. Sousa-Silva, D. S. Underwood, A. Yachmenev, and E. Zak, "The ExoMol database: Molecular line lists for exoplanet and other hot atmospheres," *J. Mol. Spec.* **327**, 73 – 94 (2016), new Visions of Spectroscopic Databases, Volume [III].
- ³⁴S. N. Yurchenko, R. J. Barber, J. Tennyson, W. Thiel, and P. Jensen, "Towards efficient refinement of molecular potential energy surfaces: Ammonia as a case study," *J. Mol. Spec.* **268**, 123–129 (2011).
- ³⁵S. N. Yurchenko, R. J. Barber, A. Yachmenev, W. Thiel, P. Jensen, and J. Tennyson, "A variationally computed $T = 300$ K line list for NH_3 ," *J. Phys. Chem. A* **113**, 11845–11855 (2009).
- ³⁶A. R. A. Derzi, T. Furtenbacher, J. Tennyson, S. N. Yurchenko, and A. G. Császár, "MARVEL analysis of the measured high-resolution spectra of $^{14}\text{NH}_3$," *J. Quant. Spectrosc. Radiat. Transfer* **161**, 117–130 (2015).
- ³⁷L. H. Coudert and E. Roueff, "Linelists for NH_3 , NH_2D , ND_2H , and ND_3 with quadrupole coupling hyperfine components," *Astron. Astrophys.* **449**, 855–859 (2006).
- ³⁸S. Belov, Š. Urban, and G. Winnewisser, "Hyperfine structure of rotation-inversion levels in the excited ν_2 state of ammonia," *J. Mol. Spec.* **189**, 1–7 (1998).
- ³⁹P. Dietiker, E. Milogiyadov, M. Quack, A. Schneider, and G. Seyfang, "Infrared laser induced population transfer and parity selection in $^{14}\text{NH}_3$: A proof of principle experiment towards detecting parity violation in chiral molecules," *J. Chem. Phys.* **143**, 244305 (2015).
- ⁴⁰R. L. Cook and F. C. de Lucia, *Am. J. Phys.* **39**, 1433–1454 (1971).
- ⁴¹All supplementary data are available online at <https://doi.org/10.5281/zenodo.855339>.
- ⁴²A. Yachmenev and A. Owens, "A general TROVE-based variational approach for rovibrational molecular dynamics in external electric fields," *J. Chem. Phys.* (2017), in preparation.
- ⁴³S. N. Yurchenko, R. J. Barber, and J. Tennyson, "A variationally computed line list for hot NH_3 ," *Mon. Not. Royal Astron. Soc.* **413**, 1828–1834 (2011).
- ⁴⁴T. H. Dunning, *J. Chem. Phys.* **90**, 1007 (1989).
- ⁴⁵R. A. Kendall, T. H. D. Jr., and R. J. Harrison, "Electron affinities of the first-row atoms revisited. Systematic basis sets and wave functions," *J. Chem. Phys.* **96**, 6796–6806 (1992).
- ⁴⁶G. E. Scuseria, "Analytic evaluation of energy gradients for the singles and doubles coupled cluster method including perturbative triple excitations: Theory and applications to FOOF and Cr_2 ," *J. Chem. Phys.* **94**, 442–447 (1991).
- ⁴⁷CFOUR, Coupled-Cluster techniques for Computational Chemistry, a quantum chemical program package written by J. F. Stanton, J. Gauss, M. E. Harding, and P. G. Szalay with contributions from A. Auer, R. J. Bartlett, U. Benedikt, C. Berger, D. E. Bernholdt, Y. J. Bomble, L. Cheng, O. Christiansen, M. Heckert, O. Heun, C. Huber, T.-C. Jagau, D. Jonsson, J. Jusélius, K. Klein, W. J. Lauderdale, D. A. Matthews, T. Metzroth, L. A. Mück, D. P. O'Neill, D. R. Price, E. Prochnow, C. Puzzarini, K. Ruud, F. Schiffmann, W. Schwalbach, S. Stopkowicz, A. Tajti, J. Vázquez, F. Wang, J. D. Watts, and the integral packages MOLECULE (J. Almlöf and P. R. Taylor), PROPS (P. R. Taylor), ABACUS (T. Helgaker, H. J. Aa. Jensen, P. Jørgensen, and J. Olsen), and ECP routines by A. V. Mitin and C. van Wüllen. For the current version, see <http://www.cfour.de>.
- ⁴⁸P. Pykkö, "Year-2008 nuclear quadrupole moments," *Mol. Phys.* **106**, 1965–1974 (2008).
- ⁴⁹L. Augustovičová, P. Soldán, and V. Špirko, "Effective Hyperfine-Structure Functions of Ammonia," *Astrophys. J.* **824**, 147 (2016).
- ⁵⁰We note that we found some inconsistencies in the experimental results reported in Table VIII of reference 39, which we have corrected in our analysis.
- ⁵¹L. Olsen, O. Christiansen, L. Hemmingsen, S. P. A. Sauer, and K. V. Mikkelsen, "Electric field gradients of water: A systematic investigation of basis set, electron correlation, and rovibrational effects," *J. Chem. Phys.* **116**, 1424–1434 (2002).
- ⁵²O. Axner, P. Kluczyński, and Å. M. Lindberg, "A general non-complex analytical expression for the n th Fourier component of a wavelength-modulated Lorentzian lineshape function," *J. Quant. Spectrosc. Radiat. Transfer* **68**, 299–317 (2001).
- ⁵³T. J. Sears, private communication (2017).
- ⁵⁴A. Yachmenev, I. Polyak, and W. Thiel, "Theoretical rotation-vibration spectrum of thioformaldehyde," *J. Chem. Phys.* **139**, 204308 (2013).
- ⁵⁵A. F. Al-Refaie, A. Yachmenev, J. Tennyson, and S. N. Yurchenko, "ExoMol line lists - VIII. a variationally computed line list for hot formaldehyde," *Mon. Not. Royal Astron. Soc.* **448**, 1704–1714 (2015).
- ⁵⁶P. Coles, S. N. Yurchenko, and J. T. Tennyson, (2017), in preparation.
- ⁵⁷D. A. Horke, Y.-P. Chang, K. Długołęcki, and J. Küpper, "Separating para and ortho water," *Angew. Chem. Int. Ed.* **53**, 11965–11968 (2014), arXiv:1407.2056 [physics].